# hiPSC-derived 3D cardiac microtissue models with integrated immune cells and vasculature

Arslan-van Bergen, U.

# Integration of hiPSC-derived macrophages into 3D cardiac microtissues




## Authors and Affiliations

Ulgu Arslan[1], Nikola Popovic[1], Kendy E. Urdaneta[1], Milica Dostanic[1], Francijna E. van den Hil[1], Richard Davis[1], Christine L. Mummery[1], Valeria Orlova[1*]

[1] Department of Anatomy and Embryology, Leiden University Medical Centre, Leiden, The Netherlands

* Corresponding author


*In preparation*

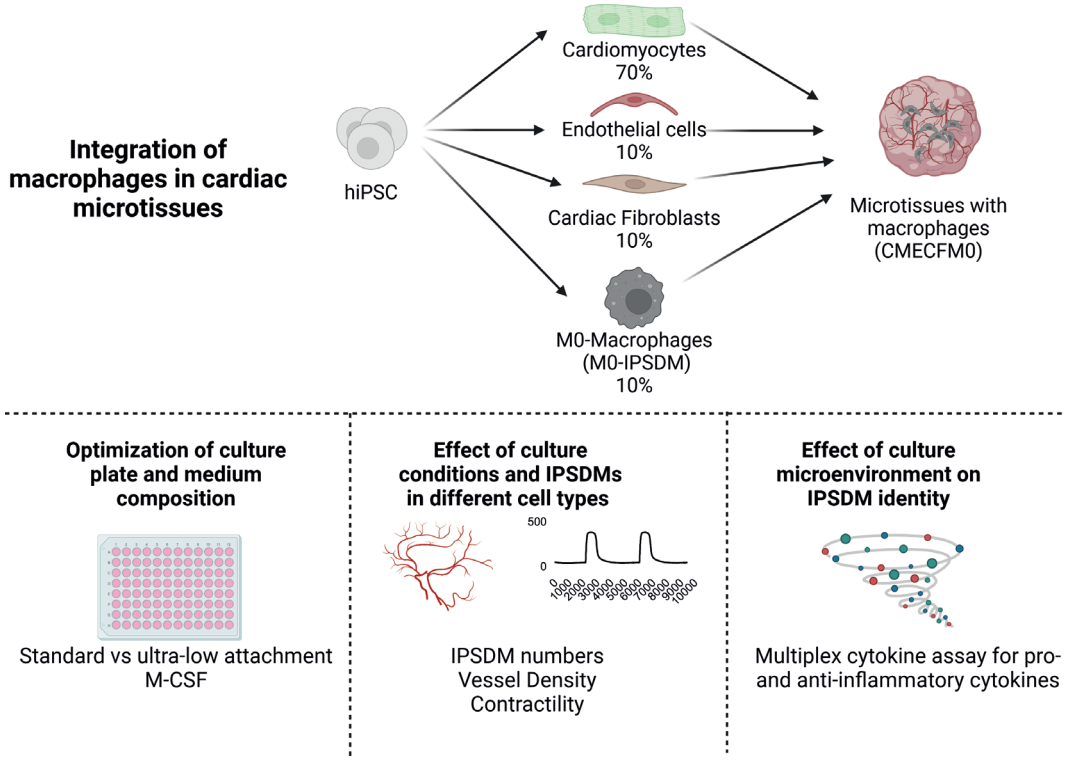


*Graphical abstract*

## Summary

Cardiac resident macrophages (CRM) play an important role in maintaining homeostasis in health and disease in the human heart. Their involvement in tissue regeneration makes them particularly interesting as a therapeutic target in the treatment of several heart disease such as myocardial infarction and consequent fibrosis. CRMs are heterogenous in their phenotype and function. Precise targeting of CRMs in *in vivo* models presents technical challenges due to the lack of specific markers and techniques to distinguish CRMs.

In this study, we developed a 3D cardiac microtissue model using human induced pluripotent stem cell (hiPSC)-derived macrophages (IPSDMs) (CMECFM0) in addition to hiPSC-derived cardiomyocytes, endothelial cells and cardiac fibroblasts. We tested various conditions such as 96-well plate types and cell culture growth medium composition to optimize the formation and maintenance of CMECFM0.

We found that adding macrophage colony-stimulating factor (M-CSF) increased the number of IPSDMs present in CMECFM0s on days 7 and 14 of the culture period, although this diminished by day 21. M-CSF supplementation did not affect vessel density or the duration of microtissue contraction. However, we did observe significant differences in the amounts of pro- and anti- inflammatory cytokines in CMECFM0s when M-CSF was added. Our study demonstrated that IPSDMs can be integrated into the cardiac microtissues under appropriate conditions without migrating out. However, we noted that an initial increase in macrophage numbers in the microtissues was not sustained and their number decreased over time. Future studies will address why the IPSDMs disappeared but, more importantly, whether they are plastic and respond to the cardiac microtissue environment by acquiring CRM-like function and identity, adding to their value as a model of inflammation in the heart.



**Keywords:**

human induced pluripotent stem cells; cardiac microtissue; macrophages.

## Introduction

The heart is one of the most important organs in the body and the interaction between the local tissue microenvironment and the different cellular components play an important role in health and disease. Among the cellular components, cardiac resident macrophages (CRMs) have emerged as one key element as they contribute to the structural integrity, function and immune response to stimuli in the heart (Zaman and Epelman, 2022; Ginhoux and Jung, 2014; Hulsmans et al., 2017; Nicolás-Ávila et al., 2020). Unlike their circulatory counterparts, CRMs are located in the heart throughout their lifetime. CRMs originate from the yolk-sac during early embryonic hematopoiesis, and are important for the maintenance of the healthy heart (Hoeffel and Ginhoux, 2015). Importantly, these yolk-sac derived CRMs

are mostly involved in the tissue regeneration and angiogenesis and upon injury, CRMs can self-renew through local proliferation (Epelman et al., 2014; Dick et al., 2019). Intriguingly, adult hematopoiesis coincides with the loss of the regenerative ability of the heart and with bone marrow-derived macrophages infiltrating the heart upon injury in animal models (Molawi et al., 2014). However, at present, knowledge on CRMs in the human heart is limited.

Several *in vitro* 3D tissue models have been established to study macrophages in various culture platforms and have shown their effect on tissue regeneration, for example in engineered skeletal muscle (Juhas et al., 2018). Other studies highlighted how the microenvironmental cues affect the phenotype and function of macrophages (Lavin et al., 2014; Saleh and Bryant, 2018; Dollinger et al., 2018). However, macrophage populations in tissues are heterogenous and are difficult to isolate and culture *in vitro* (Gordon and Plüddemann, 2017). Peripheral blood-derived macrophages are often used to study macrophage biology, but their developmental origin differs from that of tissue-resident macrophages and therefore they are not a true model of tissue-resident cells (Ginhoux and Jung, 2014). Human induced pluripotent stem cell (hiPSC)-derived macrophages appear on the basis of their developmental origin in differentiation could be an alternative cell source of tissue-resident macrophages (Lee et al., 2018). Recent studies demonstrated that hiPSC-derived macrophages promote intestine, skin and brain organoid maturation and functionality (Múnera et al., 2023; Hudaa Gopee et al., 2023; Song et al., 2024; Aktories et al., 2022). Furthermore, incorporating macrophages in the organoid system promoted the acquisition of tissue-specific macrophage characteristics. We hypothesized that a similar principle could apply to other organ models, including the heart.

Here we attempted to integrate hiPSC-derived macrophages (IPSDMs) (Cao et al., 2019) into 3D cardiac microtissues (MTs) (Giacomelli et al., 2020). We demonstrated that IPSDMs survived in 3D cardiac MTs for at least three weeks, although their numbers decreased over time. We did not observe effects of IPSDMs on the microvascular network density or contractile parameters under the conditions analyzed. We also showed that secreted cytokines can be detected in the medium collected from 3D cardiac MTs, but this requires large number of MTs as well as additional concentration step of the samples in order to reach the detection limit. We found both anti- and pro- inflammatory cytokines in the medium, indicating that IPSDMs resemble a mixed population of M2 and M1 sub-types. Additional studies addressing medium composition, macrophage number and timing will be required to advance the model such that it is suitable for studies on the role of macrophages in the healthy heart, as well as in cardiac disease modeling.

# Methods

## hiPSC lines and maintenance

Maintenance of hiPSCs were done on vitronectin-coated 6x-well plates and the medium used was TeSR-E8, all from STEMCELL Technologies, following the manufacturer's instructions. The following hiPSC lines were used in this study: LUMC0020iCTRL06 (derived from skin fibroblasts, https://hpscreg.eu/cell-line/LUMCi028-A) (Zhang et al., 2014); NIH Center for Regenerative Medicine: NCRM-1 (derived from CD34+ cord blood cells, https://hpscreg.eu/cell-line/CRMi003- A), obtained from RUDCR Infinite Biologics at Rutgers University, was modified in-house with a GFP expression cassette under the human cytomegalovirus (hCMV) early enhancer/chicken β actin (CAG) promoter using a previously established protocol (Rostovskaya et al., 2012); The Allen Cell Collection: AICS- 0061 cl.36 (derived from skin fibroblasts, https://hpscreg.eu/cell-line/UCSFi001-A-28) with mEGFP insertion site at H2B was obtained from Coriell Institute for Medical Research.



## Differentiation of cardiomyocytes

hiPSC differentiation into CM was induced in 2D monolayer as described previously (Giacomelli et al., 2017; Berg et al., 2016). Shortly, Matrigel coated plates (75 µg/ml growth factor-reduced Matrigel (Corning)) was seeded with 25 × 103 cells/cm2 on day -1. On day 0, cardiac mesoderm differentiation was induced by changing E8 to B(P)EL medium (Bovine Serum Albumin [BSA] and Essential Lipids), supplemented with a cytokine mixture (20 ng/ml BMP4, R&D Systems; 20 ng/ml ACTIVIN A, Miltenyi Biotec; 1.5 µM GSK3 inhibitor CHIR99021, Axon Medchem). After 3 days, medium was refreshed with B(P)EL supplemented with XAV939 which is a WNT inhibitor (5 µM, Tocris) and incubated for 3 days. After this, B(P)EL medium was refreshed every 3-4 days.

## Differentiation of cardiac fibroblasts

HiPSC differentiation to CFs was induced using an epicardial (EPI) monolayer differentiation protocol (Guadix et al., 2017) as a starting point (Giacomelli et al., 2020). Briefly, Matrigel coated 6x well plates was seeded with 25 × 103 cells per cm2 on day -1. On day 0, cardiac mesoderm was induced as described above. After 3 days, medium was refreshed with B(P) EL supplemented with XAV939 (5 µM), BMP4 (30 ng/ml) and Retinoic Acid (RA; 1 µM; Sigma Aldrich) and incubated for 3 days. On day 6, the medium was refreshed with B(P) EL medium supplemented with BMP4 (30 ng/ml) and RA (1 µM). On day 9, 15 × 103 per cm2 were seeded on fibronectin coated 6x-well plates (5 µg/ml of fibronectin from bovine plasma (fibronectin; Sigma Aldrich)) in B(P)EL medium supplemented with the TGFβ inhibitor SB431542 (10 µM; Tocris Bioscience). By day 12, EPIs were confluent and ready for passaging. EPI cells (30 cm2 per vial) were cryopreserved using CryoStor CS10 medium (0.5 ml/vial; Stem Cell Technologies).

EPI cryovials were used for further differentiation to CF in monolayer. Briefly, 25 × 103 EPIs were seeded per cm2 on tissue culture vitronection coated 6x well plates in B(P)EL medium supplemented with FGF2 (10 ng/ml; R&D Systems) on day 12. On day 13 and every 2 days thereafter, medium was refreshed with B(P)EL supplemented with FGF2 (10 ng/ml). On day 19, medium was changed from B(P)EL to Fibroblast Growth Medium 3 (FGM3; PromoCell) to expand CFs. FGM3 was refreshed every 2-3 days for approximately 10 days in total. Around day 29, CFs were confluent and ready to be passaged at 1:2 ratio. FGM3 was refreshed 24h after passaging and every 2-3 days thereafter. CFs (10cm2 per vial) were cryopreserved using CryoStor CS10 medium (0.5 ml/vial; Stem Cell Technologies).

## Differentiation of endothelial cells

hiPSC differentiation to ECs was induced as described previously (Orlova et al., 2014). Briefly, hiPSCs were maintained in mTeSR-E8 medium. Mesoderm was induced between day 0-3. mTeSR-E8 medium was replaced with B(P)EL medium supplemented with 8 µM CHIR99021 (Tocris Bioscience, 4423). Cells were refreshed with vascular specification medium B(P)EL supplemented with VEGF (50 ng/ml) and 10 µM SB431542 (Tocris Bioscience, 1614) at day 3, day 6, and day 9. hiPSC-ECs were isolated on day 10 and CD31-DynabeadsTM (Thermo Fisher Scientific) was used, as previously described (Orlova et al., 2014). hiPSC-ECs were expanded in complete EC growth medium (EC-CGM) comprised of Human Endothelial-serum free medium (EC-SFM) with 1% Human platelet poor serum (P2918, Sigma) and supplemented with VEGF (30 ng/ml) and bFGF (20 ng/ml), as described previously with minor modifications (Orlova et al., 2014). hiPSC-ECs were expanded for additional 3-4 days post- isolation until confluent and cryopreserved using cryopreservation medium consists of 50% fetal bovine serum, 40% EGM2 and 10% dimethyl sulfoxide at passage number 1 (P1) (StemCell Technologies, 07930).

## Differentiation to M0-IPSDMs

HiPSC differentiation to monocytes was induced following a previously established protocol (Cao et al., 2020). Shortly, hiPSCs were passaged in low ratio (10.000 cells/cm2) and maintained in mTeSR-E8 medium. On day 0, mesoderm was induced with IF9S medium supplemented with 50 ng/mL BMP4, 15 ng/mL ACTIVIN A, and 1.5 µM CHIR99021 until day 2. On day 2, medium was refreshed with IF9S supplemented with 50 ng/mL VEGF, 50 ng/mL bFGF, 50 ng/mL SCF (Miltenyi Biotec), and 10 µM SB431542. On day 5 and day 7, refreshment was done with IF9S supplemented with 50 ng/mL VEGF, 50 ng/mL bFGF, 50 ng/mL SCF, 50 ng/mL IL-6, 50 ng/mL TPO and 10 ng/mL IL-3 (all from Miltenyi Biotec). On day 9, all non-adhered cells were collected. Adherent cells were detached using TrypLE (Life Technologies) for 10 min at 37°C and combined with non-adherent cells in IF9S supplemented with 50 ng/mL IL-6, 10 ng/mL IL-3, and 80 ng/mL M-CSF (Miltenyi Biotec). 24-well ultra-low attachment plate (Corning Life Sciences) was used to seed the cells. Medium was refreshed with IF9S medium containing 50 ng/mL IL-6, 10 ng/mL IL-3, and 80 ng/mL M-CSF every 2 days after.

On day 15 non-adherent cells were collected in a tube and washed with FACS buffer (PBS, 0.5% BSA, 2 mM EDTA). Then, CD14 MicroBeads (Miltenyi Biotec) was used for CD14+ cell isolation following the manufacturer's instructions; 60 µL of MicroBeads were mixed with 1 × 107 cells. Isolated CD14+ cells were cryopreserved in CryoStor CS10 medium (STEMCELL Technologies).

To further differentiate to M0-IPSDMs , hiPSC-monocytes were thawed and plated in fetal bovine serum coated coated 2 wells of a 12-well plate in IF9S medium supplemented with 80 ng/mL M-CSF. Medium was refreshed every 2-3 days until day 7.

## 3D cardiac microtissue formation

MTs with three cell types were formed as described previously (Giacomelli et al., 2020). Prior to MT formation, hiPSC-ECs and hiPSC-CFs were prepared as follows: 3-4 days before MT formation, a vial of cryopreserved hiPSC-ECs and a vial of cryopreserved hiPSC-CFs were thawed and cultured either in EC-CGM on plates coated with gelatin (hiPSC-ECs), or in FGM3 on uncoated plates (hiPSC-CFs). HiPSC- CMs were thawed on Matrigel coated 12x well plate 5 days prior to MT formation day. M0-IPSDMs were thawed on overnight FBS coated 12x well plate in IF9S medium as previously described (Cao et al., 2020). On the day of MT formation (day 0), hiPSC-ECs and hiPSC-CFs were detached using TrypLE 1X for 2-3 mins at RT (EC) and 5 mins at 37 °C, 5 % CO2 (CF), centrifuged for 3 min at 1100 rpm, resuspended in B(P)EL medium and counted. hiPSC-CMs were dissociated using the TryplE 5X for 10 mins at 37°C, 5 % CO2, resuspended in B(P)EL medium and counted. M0-IPSDMs were dissociated using tryplE 1X for 5 mins at 37 °C, 5 % CO2, centrifuged for 3 min at 1100 rpm, resuspended in B(P)EL medium and counted. Cell suspensions for CMECF were combined to a total of 5000 cells (70% CM, 15 % EC and 15 % CF (CMECF) or 70 % CM, 10 % EC, 10 % CF and 10 % M0-IPSDMs (CMECFM0)) per 50 µl B(P)EL medium supplemented with VEGF (50 ng/ml) and FGF2 (5 ng/ml). Cell suspensions for CMECFM0 were combined to a total of 5000 cells (70 % CM, 10 % EC, 10 % CF and 10 % M0-IPSDMs) per 70 µl B(P)EL medium supplemented with VEGF (50 ng/ml), FGF2 (5 ng/ml) and M- CSF (80 ng/ml). For all MTs, cell suspensions were seeded either on standard V-bottom 96-well microplates (Greiner bio-one, 651161) and standard U-bottom (Greiner bio-one, 650161) or ultra- low attachment U- bottom 96-well microplates (ThermoFisher NunClon Sphera Treated, 174925) and centrifuged for 10 min at 1100 rpm. MTs were incubated at 37 °C, 5 % CO2 for 21 days with media refreshed every 3-4 days.

## Immunofluorescence imaging

On day 7, 14 and 21, CMECFM0s were fixed using 4 % paraformaldehyde (PFA) for 1 h at 4 °C. Permeabilization was done using PBS(-) supplemented with 0.2 % TritonX-100 for 30 mins at RT. Then, PBS(-) supplemented with 10% fetal bovine serum (FBS) was used for blocking for at least 2 h at RT. Primary antibodies of CD68 (ThermoFisher Scientific), ACTN2 (Sigma Aldrich cat no: A7811) and CD31 (R&D Systems, cat no: AF806) was added in

blocking solution described previously and added on CMECM0 overnight at 4 °C. Secondary antibodies of donkey anti rabbit IgG, highly crossed absorbed antibody with Alexa Fluor 594 (ThermoFisher, cat no: A21206), donkey anti-mouse IgG, highly crossed absorbed antibody with Alexa Fluor 594 (ThermoFisher, cat no: A21203), donkey anti sheep IgG, highly crossed absorbed antibody with Alexa Fluor 647 (ThermoFisher, cat no: A21448) were added in blocking solution on CMECFM0 overnight at 4 °C. After each step, 3x PBS(-) wash for 20 mins was followed. After the DAPI staining (in PBS(-)), MTs were resuspended in ProLong Gold (ThermoFisher) and transferred on microscopy slides (VWR, 631-1553). Coverslips were used to mount MTs in slides. Confocal images were captured to create 3D stack using Andor Dragonfly spinning disk confocal microscope using a 40x or 63x objective. Image processing was done using Imaris 9.5 software (Bitplane, Oxford Instruments).

## Characterization of vessel density and macrophage number in 3D

Whole MT images of CMECFM0 were captured using ImageXpress Micro confocal high-content imaging microscopy (Molecular Devices) using 10x objective and were then quantified for vessel density and macrophage counting using pipelines developed on the free open source CellProfiler software (https://cellprofiler.org/) (Vila Cuenca et al., 2021; Carpenter et al., 2006). Briefly, pre- processing steps enhanced image features in all images. A Gaussian filter to reduce non-specific object identification was done. Two filter steps of images of vascular density were applied to reduce non-specific segmentation from cell junctions and a minimum cross-entropy thresholding method was used to produce a binary image.

## Contraction analysis

For pacing experiments, custom-made electrodes were used. MTs were stimulated at 1.2Hz with 10V/cm strength and 10 ms long stimulation pulse. Movies of spontaneous beating or paced MTs from CMECF and CMECFM0 conditions were acquired until 2-3 beats were captured at 37 °C. ThorLabs DCC3240M camera (Leica Inverted microscope IBDE), using the ThorLabs uc480 software (v 4.20), at 37 °C and 5 % CO2 at 100 frames/s and a 10x objective phase contrast objective was used for recordings. MUSCLEMOTION ImageJ macro (ImageJ v. 2.0.0-rc-49) was used to analyze recordings as described previously (Sala et al., 2018).

## Multiplexed Cytokine Assay

MTs were refreshed 4 days prior to medium collection. For this, the medium in the wells was completely aspirated and 40 µl of fresh medium was added into each well. MTs were not disturbed the next 4 days until medium collection. After 4 days, the medium from 40 MTs from CMECF, CMECFM0 -M-CSF and CMECFM0 +M-CSF were collected and stored at -80 oC. On the day of the multiplex cytokine bead assay, collected medium was thawed two hours prior to the experiment. Samples were concentrated using PierceTM Protein Concentrators PES (ThermoFisher) following manufacturer's instructions.
Concentration of cytokines (IL-12p70, TNF-α, IL-6, IL-4, IL-10, IL-1β, Arginase, TARC, IL-1RA,

IL-12p40, IL-23, IFN-γ and IP-10) was measured using a LEGENDplex human macrophage/microglia Panel kit (13-plex) (BioLegend, cat no: 740511) according to the manufacturer's instructions. Samples were run on Cytek 3-Laser Aurora spectral flow cytometer (Cytek Biosciences, USA).

### Statistical Analysis

GraphPad Prism 9 was used to perform statistical tests. Two-way ANOVA was applied as appropriate to test for differences in means between groups/conditions. Data are expressed and plotted as the Mean ± SD, except figure 4D-G which was plotted as the Mean ± SEM as indicated in figure legend. Detailed statistics and exact P-values are indicated in each figure legend. Statistical significance was defined as $P < 0.05$.

## Results



### Integration of M0-IPSDMs in 3D cardiac MTs

In order to integrate M0-IPSDMs in cardiac MTs, we first adapted a previously published protocol (Giacomelli et al. al., 2020) with keeping the percentage of CMs at 70%. Cardiac MTs with M0-IPSDMs (CMECFM0) were formed using the following predefined cell percentages: 70% CMs, 10 % ECs, 10 % CFs and 10 % M0-IPSDMs in B(P)EL medium that was additionally supplemented with VEGF (50 ng/ml), FGF2 (5 ng/ml) and M-CSF (80 ng/ml) (Figure 1A). On day 3 of MT formation, CMECFM0 (Figure 1C) were compared to MTs without IPSDMs (CMECF, Figure 1B). Both conditions formed compact MTs. However, we observed that in CMECFM0, IPSDMs appeared to be attracted by dead cells that surrounded MTs and they migrated outside of MTs, clearing-up the dead cells. We also noted that some IPSDMs attached to the bottom of the well. CMECFM0s were maintained for 21 or 31 days in culture with medium refreshment every 3-4 days. At the end of day 21 and 31, we performed immunofluorescent staining of CMECFM0s to visualize cellular subsets (Figure 1D and E, respectively). hiPSC-CMs were homogenously distributed and hiPSC-ECs self-organized into microvascular networks in day 21 and day 31 CMECFM0s. IPSDMs were evident in MTs on day 21 and 31; however, their number seemed to be higher in day 31 CMECFM0s (Figure 1E). Interestingly, IPSDMs appeared to localize close to microvascular networks.

### Ultra-low attachment plates support retaining macrophages inside 3D cardiac MTs

In order to track the IPSDMs inside of MTs, we generated CMECFM0 with M0-IPSDMs from a fluorescent reporter line (NCRM1-GFP). We next compared the standard and ultra-low attachment U- bottom plates (Figure 2A). We observed that in standard U-bottom plates, IPSDMs migrated outside of MTs, as evidenced by a green fluorescent signal (Figure 2B). On the other hand, ultra-low attachment U-bottom plates prevented IPSDM migration outside of the CMECFM0. CMECFM0s were maintained until day 21 either in regular MT medium without M-CSF (-M-CSF) or with M-CSF (+M- CSF).

## Figure 1

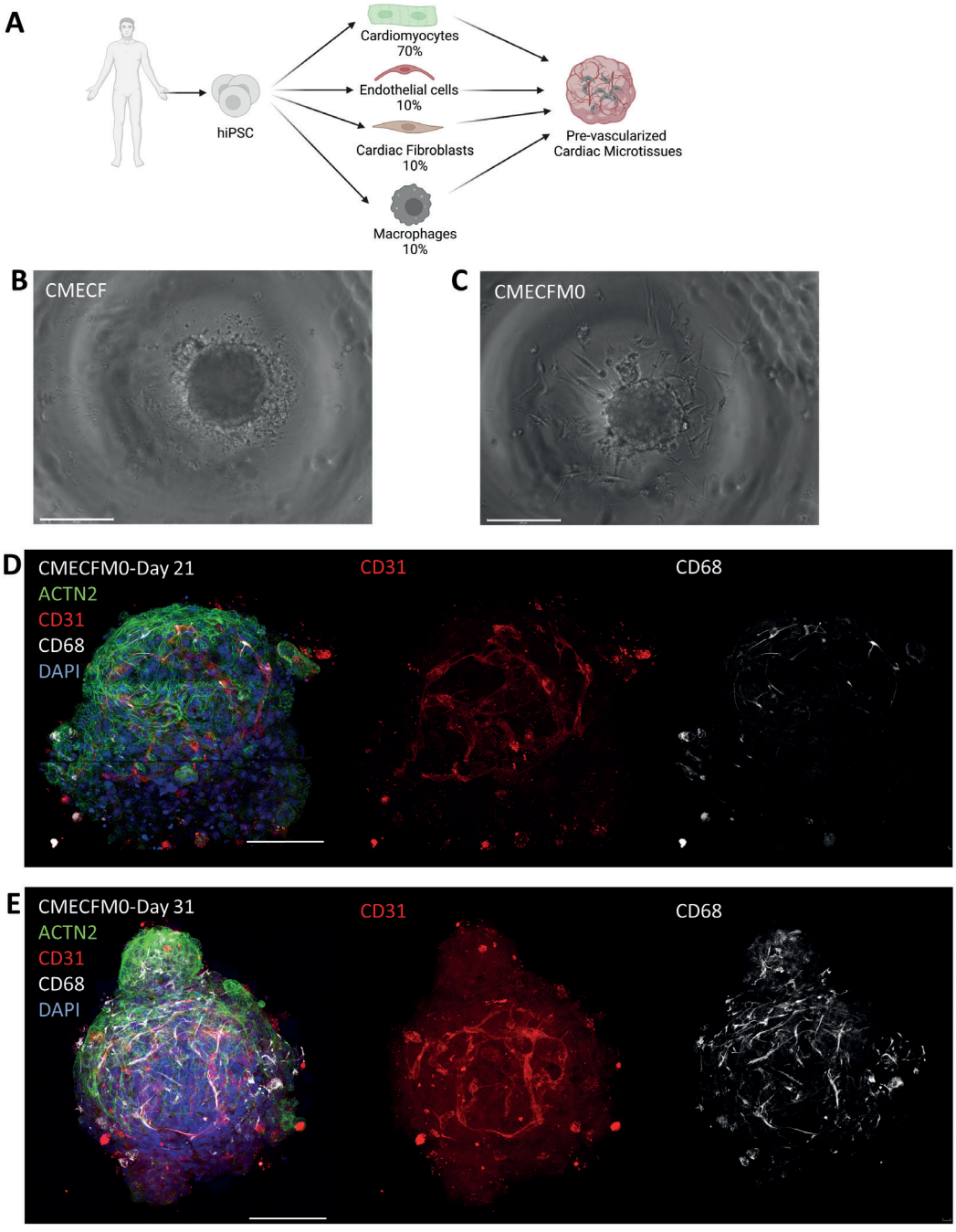


***Figure 1: Integration of M0-IPSDMs in cardiac MTs.*** *(A) Schematic showing cellular composition of cardiac MTs with M0-IPSDMs with respective cell percentages indicated. (B, C) Representative bright-field images of cardiac MTs without IPSDMs (CMECF) (B) and with IPSDMs (CMECFM0) (C). (D, E) Immunofluorescence staining of CMECFM0 on day 21 (D) and day 31 (E) showing ACTN2 in green, CD31 in red and CD68 in white. Scale bars: 275 um (B-C), 100 um (D-E).*

**Figure 2**

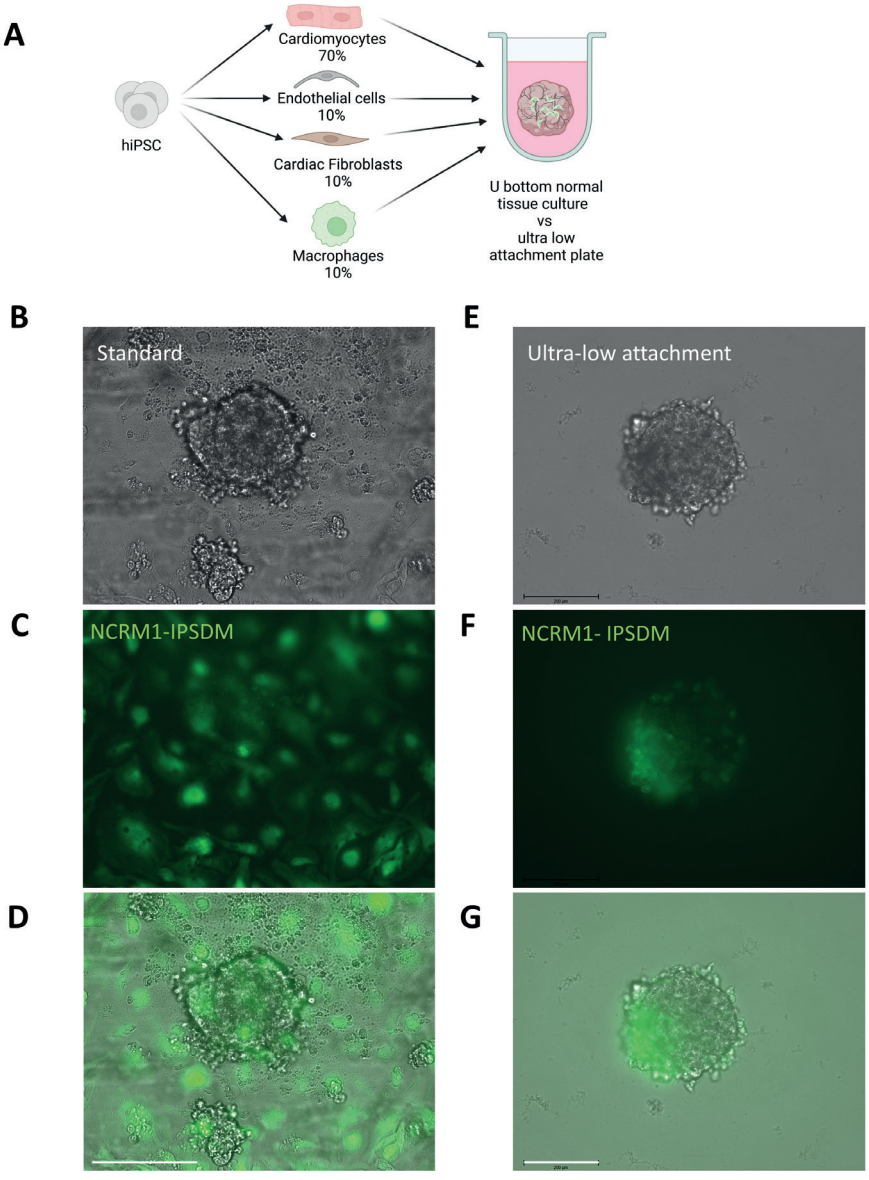


***Figure 2: Optimization of the formation of CMECFM0s.*** *(A) Schematic showing formation of CMECFM0s in U-bottom plates. (B-G) Representative images of CMECFM0 after 21 days of formation in standard U-bottom plates (B-D) or ultra-low attachment U- bottom plates (E-G). Bright-field images of CMECFM0 are shown in B, E; M0-IPSDMs differentiated from generically encoded fluorescent hiPSC line (NCRM1-GFP) are shown after integration in cardiac MTs (in green) (C, F); Merged imaged are shown in D, G. Scale bars: 200 µm.*

## Characterization of 3D cardiac MTs with M0-IPSDMs

To quantify the total number of IPSDMs at different timepoints, and also study the effect of M-CSF supplementation, we differentiated macrophages from H2B-GFP nuclear fluorescent reporter hiPSC line (Allen Institute, AICS-0061-036) (Roberts et al., 2017). Confocal imaging of CMECFM0s on day 7 (Figure 3A), 14 (Figure 3B) and 21 (Figure 3C) showed homogenous distribution of M0-IPSDMs, identified by H2B-GFP positive nuclei and CD68 immunostaining, ACTN2 positive hiPSC-CMs, and self- organized microvasculature formed by CD31 positive hiPSC-ECs.

We next quantified the total number of H2B-GFP positive IPSDM in CMECFM0s with and without M- CSF supplementation at day 7, 14 and 21. M-CSF supplementation resulted in more IPSDMs at day 7 and 14, but not 21 after MT formation (Figure 4A). The total number of IPSDM decreased overtime in both conditions, indicating that M-CSF supported macrophage proliferation at early stages of MT formation, but had no effect upon a prolonged culture. Quantification of microvascular networks and contractile parameters showed comparable vessel density between different conditions (Figure 4B) and no difference in contraction duration upon pacing at 1.2 Hz (Figure 4C), respectively.

Finally, we examined cytokine secretion using a multiplex assay (macrophage/microglia cytokine panel) that includes both pro- and anti-inflammatory cytokines. We were only able to detect some of the cytokines that could potentially be measured in the assay in CMECFM0s, and not in control MTs (CMECF). Specifically, IL-10, IL-6, IP-10 and IL-1RA were measured but IL-10, IL-6 levels were negligibly low (14.04±3.947 pg/ml and 191.4±92.93 pg/ml, respectively, mean±SEM) (Figure 4D, F). IP-10 and IL-1RA showed the highest expression in CMECFM0 with M-CSF supplementation, although IL-1RA was 10-fold higher than IP-10, suggesting that majority of IPSDMs acquired M2-like identity and only a minor subset of IPSDMs acquired M1-like identity (Figure 4E, G).

## Discussion

In the present study, we optimized and characterized several culture conditions to integrate M0- IPSDMs into 3D cardiac MTs. hiPSC-derived cells; CMs, ECs, CFs and macrophages were combined in a pre-defined ratio (70% CM and 10% each non-CM cell types) in a regular V-bottom 96-well plates. CMECFM0s were compact and formed reproducibly. However, some cells migrated outside the MTs. These migratory cells were not present in CMECF which suggested that they were M0-IPSDMs. Importantly, there were dead cells surrounding MTs in CMECF condition. However, these dead cells were not present in CMECFM0 which might suggest efferocytosis by M0-IPSDMs as previously shown (Cao et al., 2019). Although we observed that some IPSDMs migrated outside, confocal images of CMECFM0 on day 21 and 31 showed that some remained in the MTs. At both time points, IPSDMs were close to the microvascular structures which is in line with the previous literature suggesting one of the niches of CRMs are vessels (Moore et al., 2017; Zaman and Epelman, 2022).

**Figure 3**

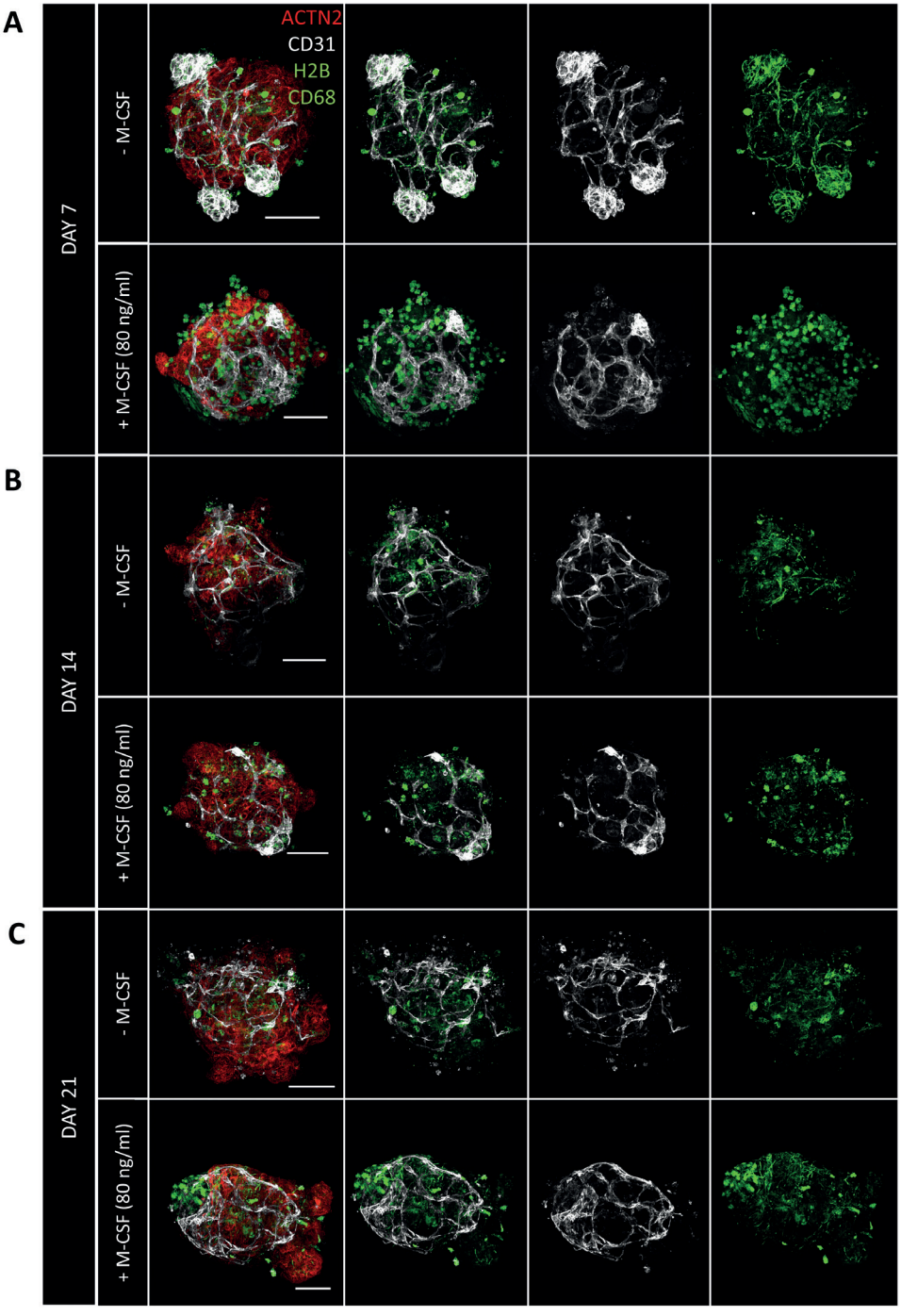


***Figure 3: Cellular composition of CMECFM0s.*** *(A-C) Representative immunofluorescent images of CMECFM0s at different days after formation with and without M-CSF (80 ng/ml) supplementation: day 7 (A), day 14 (B) and day 21 (C). Cardiomyocytes are stained with anti-ACTN2 (red), ECs are stained with anti-CD31 (gray), M0-IPSDMs are differentiated from H2B-GFP reporter hiPSC-line and additionally stained with anti-CD68 (green). Scale bars: 100 μm.*

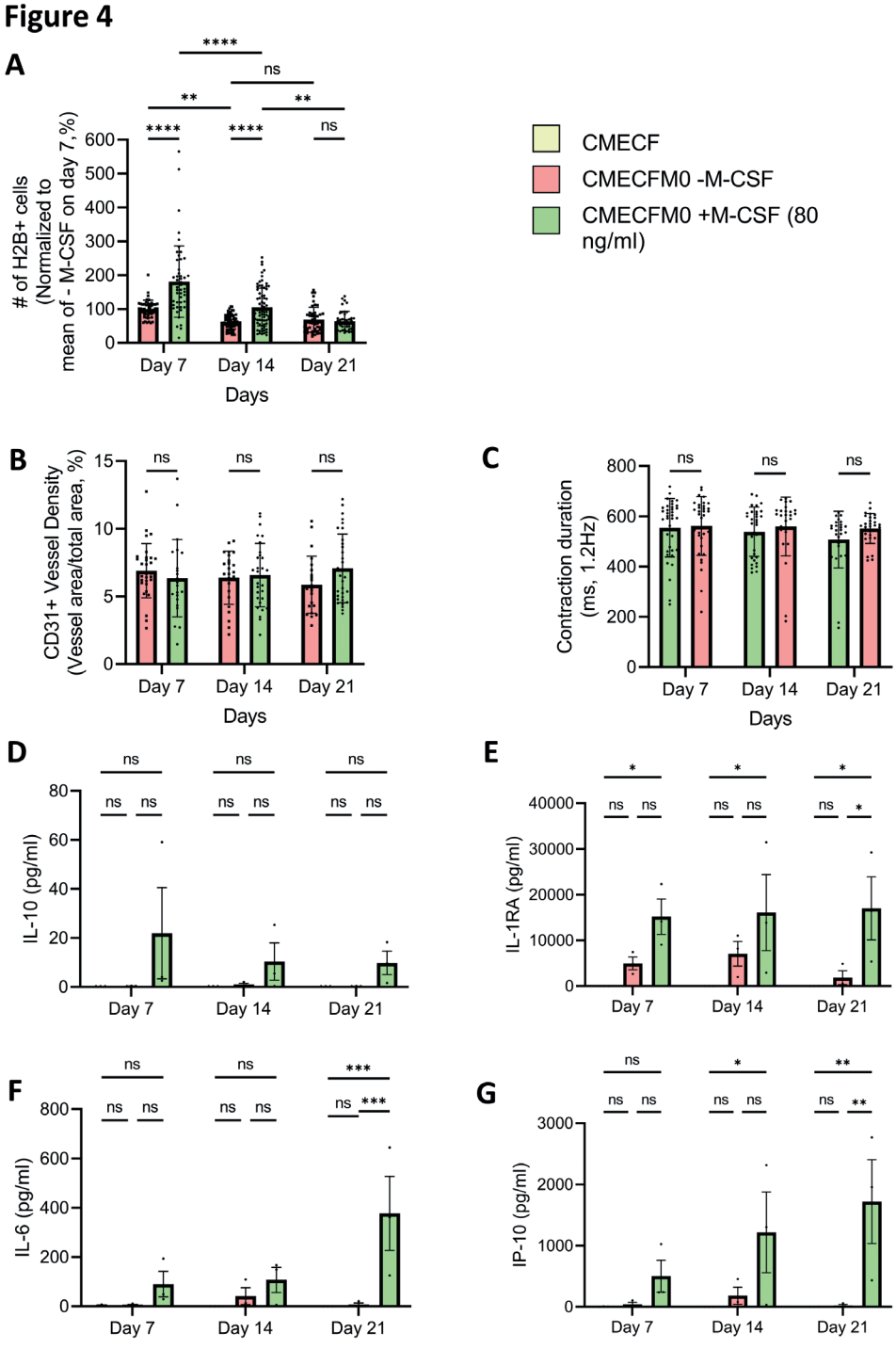


***Figure 4: Characterization of CMECFM0s.*** *(A)Quantification of the total number of M0-IPSDMs differentiated from H2B-GFP reporter hiPSC line in CMECFM0s at day 7, 14 and 21 after formation with and without M-CSF (80 ng/ml) supplementation. n>44 from 3 independent experiment. Error bars are shown in mean±SD (B) Quantification of vessel density in CMECFM0s at day 7, 14 and 21 after formation with and without M-CSF (80 ng/ml) supplementation. n>22 from 3 independent experiment. Error bars are shown in mean±SD (C) Quantification*

*of the contraction duration of CMECFM0s at day 7, 14 and 21 after formation with and without M-CSF (80 ng/ml) supplementation. CMECFM0s were paced at 1.2 Hz. n>26 from 3 independent experiment. Error bars are shown in mean±SD (D-G) Quantification of secreted cytokines by a Multiplex assay in concentrated supernatants collected on day 7, 14 and 21 after 4 days upon medium refresh. Medium is collected from n= 40 MTs for each condition from 3 independent experiments. Yellow bars: CMECF, pink bars: CMECFM0 -M-CSF, green bars: CMECFM0 +M-CSF. Error bars (D-G) are shown as mean±SEM. *p < 0.5,**p < 0.01,***p < 0.001; ns, not significant.*

To prevent cell migration in the CMECFM0 condition, we tested other types of cell culture plates. In the regular CMECF condition, we usually use V bottom plates to seed the cells and these plates are centrifuged to sediment cells in the bottom as a compact cluster (Campostrini et al., 2021). This could perhaps increase cell death as the MTs become attached to the bottom of the wells. In an attempt to decrease cell death, we first changed the plates from V- to U-bottom using the same brand of standard 96-microwell plates. However, migratory cells were still present in these plates. Using a fluorescent hiPSC reporter line with nuclear tagging to generate M0-IPSDMs and integrate them in CMECFM0 confirmed the IPSDM identity of migratory cells. However, when we used ultra- low attachment plates, migration of cells was completely prevented and M0-IPSDMs remained in the MTs.



Previously, CMECF was generated and maintained in the MT medium (Giacomelli et al., 2020). In CMECFM0, M-CSF was supplemented in the MT medium in an attempt to enhance M0-IPSDM survival and proliferation as reported in previous studies (Otero et al., 2009). Confocal imaging of these MTs at different time points (day7, 14 and 21) showed that IPSDMs were more homogenously distributed in the MTs at the earlier time points. However, they remained in close proximity to the microvasculature which was formed by self-organization of hiPSC-ECs throughout the culture period. The number of H2B+ IPSDM increased on day 7 and 14 in CMECFM0 +M-CSF compared to -M-CSF. However, surprisingly, they were comparable on day 21 in terms of IPSDM number. In addition, there was a significant decrease in IPSDM numbers later in the culture period. This could be partly due to the MT medium as it had not been optimized for M0-IPSDMs.

To examine the effect of IPSDM on other cellular subsets, we quantified microvascular network density and contractile parameters of cardiac MTs with and without M-CSF supplementation. Despite increased IPSDM numbers upon M-CSF supplementation, we observed had no effect on the total vascular network density. This was surprising as earlier studies demonstrated that macrophages support formation of vascular networks *in vitro* and *in vivo* (Krishnasamy et al., 2017; Gamrekelashvili et al., 2016; Moore et al., 2017). In addition, contraction duration was comparable between CMECFM0 -M-CSF and +M-CSF on day 7, 14 and 21, and did not change over time. It would be interesting to investigate whether IPSDMs have an effect on electrophysiological properties or force of contraction of cardiomyocytes in the future.

To characterize the IPSDM phenotype in the CMECFM0 microenvironment, we collected medium samples to determine the cytokine release in each condition. We showed that secretion of anti- inflammatory cytokine IL-1RA was higher in CMECFM0s supplemented with M-CSF. We also detected some levels of pro-inflammatory cytokine IP-10 in

CMECFM0s supplemented with M-CSF, although it was 10-fold lower compared to IL-1RA. Surprisingly, an increase in cytokine secretion upon M-CSF supplementation did not correlate with the overall decrease in the total IPSDM number, indicating that M-CSF could promote macrophage polarization in 3D cardiac MTs. It would be interesting to characterize macrophage polarization at the single cell resolution in the future either by immunofluorescent staining or by flow cytometry using specific M1 and M2 markers or single-cell RNA sequencing.

In summary, here we optimized culture conditions to integrate M0-IPSDMs into 3D cardiac MTs. We showed that M-CSF supplementation in the medium increased IPSDM numbers at the early time points. In addition, M-CSF or IPSDMs did not have any effect on vessel density or contraction duration parameters. Integration of IPSDMs resulted in upregulation of IL-1RA and IP-10 that are anti- and pro-inflammatory cytokines respectively. Although these results suggest that the MT microenvironment affects IPSDM identity, more specific assays will be necessary to characterize them further. This platform offers potential to study M0-IPSDMs in specific tissue microenvironment to better understand their involvement in health and disease.

## Acknowledgements

We thank LUMC confocal imaging facility during imaging and the Allen Cell Collection (from Coriell Institute for Medical Research), for hiPSC lines. Images were made using Biorender.com.

This work was supported by the LymphChip project with project number NWA-ORC 2019 1292.19.019 of the NWA research program 'Research on Routes by Consortia (ORC)', which is funded by the Netherlands Organization for Scientific Research (NWO); The Novo Nordisk Foundation Center for Stem Cell Medicine is supported by Novo Nordisk Foundation grants (NNF21CC0073729).

## References

Aktories, P., Petry, P., Glatz, P., Andrieux, G., Oschwald, A., Botterer, H., Gorka, O., Erny, D., Boerries, M., Henneke, P., et al. 2022. *An improved organotypic cell culture system to study tissue- resident macrophages ex vivo.* Cell Reports Methods 26;2(8):100260.

Berg, C. W. van den, Elliott, D. A., Braam, S. R., Mummery, C. L., and Davis, R. P. 2016. *Differentiation of Human Pluripotent Stem Cells to Cardiomyocytes Under Defined Conditions.* Methods in molecular biology (Clifton, N.J.) 1353:163–180.

Campostrini, G., Meraviglia, V., Giacomelli, E., van Helden, R. W. J., Yiangou, L., Davis, R. P., Bellin, M., Orlova, V. V., and Mummery, C. L. 2021. *Generation, functional analysis and applications of isogenic three-dimensional self-aggregating cardiac microtissues from human pluripotent stem cells.* Nature Protocols 16(4):2213-2256.

Cao, X., van den Hil, F. E., Mummery, C. L., and Orlova, V. V. 2020. *Generation and Functional Characterization of Monocytes and Macrophages Derived from Human Induced Pluripotent Stem Cells.* Current Protocols in Stem Cell Biology 52(1):e108.

Cao, X., Yakala, G. K., van den Hil, F. E., Cochrane, A., Mummery, C. L., and Orlova, V. V. 2019. *Differentiation and Functional Comparison of Monocytes and Macrophages from hiPSCs with Peripheral Blood Derivatives.* Stem Cell Reports 12(6):1282-1297.

Carpenter, A. E., Jones, T. R., Lamprecht, M. R., Clarke, C., Kang, I. H., Friman, O., Guertin, D. A., Chang, J. H., Lindquist, R. A., Moffat, J., et al. 2006. *CellProfiler: image analysis software for identifying and quantifying cell phenotypes.* Genome Biology 7(10):R100.

Dick, S. A., Macklin, J. A., Nejat, S., Momen, A., Clemente-Casares, X., Althagafi, M. G., Chen, J., Kantores, C., Hosseinzadeh, S., Aronoff, L., et al. 2019. *Self-renewing resident cardiac macrophages limit adverse remodeling following myocardial infarction.* Nature Immunology 20(1):29-39.

Dollinger, C., Ciftci, S., Knopf-Marques, H., Guner, R., Ghaemmaghami, A. M., Debry, C., Barthes, J., and Vrana, N. E. 2018. *Incorporation of resident macrophages in engineered tissues: Multiple cell type response to microenvironment controlled macrophage-laden gelatine hydrogels.* Journal of Tissue Engineering and Regenerative Medicine 12(2):330-340.

Epelman, S., Lavine, K. J., Beaudin, A. E., Sojka, D. K., Carrero, J. A., Calderon, B., Brija, T., Gautier, E. L., Ivanov, S., Satpathy, A. T., et al. 2014. *Embryonic and adult-derived resident cardiac macrophages are maintained through distinct mechanisms at steady state and during inflammation.* Immunity 40(1):91-104.

Gamrekelashvili, J., Giagnorio, R., Jussofie, J., Soehnlein, O., Duchene, J., Briseño, C. G., Ramasamy, S. K., Krishnasamy, K., Limbourg, A., Kapanadze, T., et al. 2016. *Regulation of monocyte cell fate by blood vessels mediated by Notch signalling.* Nature Communications 7:12597.

Giacomelli, E., Bellin, M., Orlova, V. V, and Mummery, C. L. 2017. *Co-Differentiation of Human Pluripotent Stem Cells-Derived Cardiomyocytes and Endothelial Cells from Cardiac Mesoderm Provides a Three-Dimensional Model of Cardiac Microtissue.* Current protocols in human genetics 95:21.9.1-21.9.22.

Giacomelli, E., Meraviglia, V., Campostrini, G., Cochrane, A., Cao, X., van Helden, R. W. J., Krotenberg Garcia, A., Mircea, M., Kostidis, S., Davis, R. P., et al. 2020. *Human-iPSC-Derived Cardiac Stromal Cells Enhance Maturation in 3D Cardiac Microtissues and Reveal Non-cardiomyocyte Contributions to Heart Disease.* Cell Stem Cell 26:862-879.e11.

Ginhoux, F., and Jung, S. 2014. *Monocytes and macrophages: developmental pathways and tissue homeostasis.* Nature Reviews Immunology 14:392–404.

Gordon, S., and Plüddemann, A. 2017. *Tissue macrophages: Heterogeneity and functions.* BMC Biology 15(1):53.

Guadix, J. A., Orlova, V. V, Giacomelli, E., Bellin, M., Ribeiro, M. C., Mummery, C. L., Pérez-Pomares, J. M., and Passier, R. 2017. *Human Pluripotent Stem Cell Differentiation into Functional Epicardial Progenitor Cells.* STEMCR 9:1754–1764.

Hoeffel, G., and Ginhoux, F. 2015. *Ontogeny of tissue-resident macrophages.* Frontiers in Immunology 6:486.

Hudaa Gopee, N., Huang, N., Olabi, B., Admane, C., Rose Foster, A., Torabi, F., Winheim, E., Sumanaweera, D., Miah, M., Stephenson, E., et al. 2023. *A human prenatal skin cell atlas reveals immune cell regulation of skin morphogenesis 1.* Biorxiv.

Hulsmans, M., Clauss, S., Xiao, L., Aguirre, A. D., King, K. R., Hanley, A., Hucker, W. J., Wülfers, E. M., Seemann, G., Courties, G., et al. 2017. *Macrophages Facilitate Electrical Conduction in the Heart.* Cell 169(3):510-522.e20.

Juhas, M., Abutaleb, N., Wang, J. T., Ye, J., Shaikh, Z., Sriworarat, C., Qian, Y., and Bursac, N. 2018. *Incorporation of macrophages into engineered skeletal muscle enables enhanced muscle regeneration.* Nature Biomedical Engineering 2(12):942-954.

Krishnasamy, K., Limbourg, A., Kapanadze, T., Gamrekelashvili, J., Beger, C., Häger, C., Lozanovski, V. J., Falk, C. S., Napp, L. C., Bauersachs, J., et al. 2017. *Blood vessel control of macrophage maturation promotes arteriogenesis in ischemia.* Nature Communications 8(1):952.

Lavin, Y., Winter, D., Blecher-Gonen, R., David, E., Keren-Shaul, H., Merad, M., Jung, S., and Amit, I. 2014. *Tissue-resident macrophage enhancer landscapes are shaped by the local microenvironment.* Cell 159(6):1312-26.

Lee, C. Z. W., Kozaki, T., and Ginhoux, F. 2018. *Studying tissue macrophages in vitro: are iPSC-derived cells the answer?* Nature Reviews Immunology 8(11):716-725.

Molawi, K., Wolf, Y., Kandalla, P. K., Favret, J., Hagemeyer, N., Frenzel, K., Pinto, A. R., Klapproth, K., Henri, S., Malissen, B., et al. 2014. *Progressive replacement of embryo-derived cardiac macrophages with age.* Journal of Experimental Medicine 211(11):2151-8.

Moore, E. M., Ying, G., and West, J. L. 2017. *Macrophages Influence Vessel Formation in 3D Bioactive Hydrogels.* Advanced Biosystems 1, 1600021.

Múnera, J. O., Kechele, D. O., Bouffi, C., Qu, N., Jing, R., Maity, P., Enriquez, J. R., Han, L., Campbell, I., Mahe, M. M., et al. 2023. *Development of functional resident macrophages in human pluripotent stem cell-derived colonic organoids and human fetal colon.* Cell Stem Cell 30:1434- 1451.e9.

Nicolás-Ávila, J. A., Lechuga-Vieco, A. V., Esteban-Martínez, L., Sánchez-Díaz, M., Díaz-García, E., Santiago, D. J., Rubio-Ponce, A., Li, J. L. Y., Balachander, A., Quintana, J. A., et al. 2020. *A Network of Macrophages Supports Mitochondrial Homeostasis in the Heart.* Cell 183(1):94- 109.e23 .

Orlova, V. V., Van Den Hil, F. E., Petrus-Reurer, S., Drabsch, Y., Ten Dijke, P., and Mummery, C. L. 2014. *Generation, expansion and functional analysis of endothelial cells and pericytes derived from human pluripotent stem cells.* Nature Protocols 9(6):1514-31.

Otero, K., Turnbull, I. R., Poliani, P. L., Vermi, W., Cerutti, E., Aoshi, T., Tassi, I., Takai, T., Stanley, S. L., Miller, M., et al. 2009. *Macrophage colony-stimulating factor induces the proliferation and survival of macrophages via a pathway involving DAP12 and β-catenin.* Nature Immunology 10(7):734-43 .

Roberts, B., Haupt, A., Tucker, A., Grancharova, T., Arakaki, J., Fuqua, M. A., Nelson, A., Hookway, C., Ludmann, S. A., Mueller, I. A., et al. 2017. *Systematic gene tagging using CRISPR/Cas9 in human stem cells to illuminate cell organization.* Molecular Biology of the Cell 28(21):2854-2874.

Rostovskaya, M., Fu, J., Obst, M., Baer, I., Weidlich, S., Wang, H., Smith, A. J. H., Anastassiadis, K., and Francis Stewart, A. 2012. *Nucleic Acids Research* 40(19):e150.

Sala, L., van Meer, B. J., Tertoolen, L. G. J., Bakkers, J., Bellin, M., Davis, R. P., Denning, C., Dieben, M. A. E., Eschenhagen, T., Giacomelli, E., et al. 2018. *Musclemotion: A versatile open software tool to quantify cardiomyocyte and cardiac muscle contraction in vitro and in vivo.* Circulation Research 122(3):e5-e16 .

Saleh, L. S., and Bryant, S. J. 2018. *The host response in tissue engineering: Crosstalk between immune cells and cell-laden scaffolds.* Current Opinion in Biomedical Engineering 6:58-65.

Song, A. T., Sindeaux, R. H. M., Li, Y., Affia, H., Agnihotri, T., Leclerc, S., van Vliet, P. P., Colas, M., Guimond, J.-V., Patey, N., et al. 2024. *Developmental role of macrophages modeled in human pluripotent stem cell-derived intestinal tissue.* Cell Reports 43:113616.

Vila Cuenca, M., Cochrane, A., van den Hil, F. E., de Vries, A. A. F., Lesnik Oberstein, S. A. J., Mummery, C. L., and Orlova, V. V. 2021. *Engineered 3D vessel-on-chip using hiPSC-derived endothelial- and vascular smooth muscle cells.* Stem Cell Reports 16(9):2159-2168.

Zaman, R., and Epelman, S. 2022. *Resident cardiac macrophages: Heterogeneity and function in health and disease.* Immunity 55(9):1549-1563 .

Zhang, M., D'Aniello, C., Verkerk, A. O., Wrobel, E., Frank, S., Ward-Van Oostwaard, D., Piccini, I., Freund, C., Rao, J., Seebohm, G., et al. 2014. *Recessive cardiac phenotypes in induced pluripotent stem cell models of Jervell and Lange-Nielsen syndrome: Disease mechanisms and pharmacological rescue.* Proceedings of the National Academy of Sciences of the United States of America 111(50):E5383-92.